Communication between Porphyrin Rings in the Butadiyne-Bridged Dimer Ni(OEP)(μ-C_4)Ni(OEP): A Density Functional Study

Robert Stranger,*,† John E. McGrady,† Dennis P. Arnold,‡ Ian Lane,§ and Graham A. Heath||

Department of Chemistry, Faculties, The Australian National University, Canberra, ACT 0200, Australia, Centre for Instrumental and Developmental Chemistry, Queensland University of Technology, Brisbane, QLD 4001, Australia, Centre for Magnetic Resonance, University of Queensland, Brisbane, QLD 4072, Australia, and Research School of Chemistry, The Australian National University, Canberra, ACT 0200, Australia

Received August 20, 1996[⊗]

The electronic structure and spectra of a family of nickel porphyrin complexes are analyzed using approximate density functional theory (DFT). The three complexes, Ni(OEP), Ni(OEP-C_4SiMe_3), and Ni(OEP)(μ-C_4)Ni-(OEP) represent a logical increase in complexity starting from a simple metalloporphyrin. The spectra of the three complexes all show similar features: an intense Soret band above 20 000 cm^{-1} with a weaker Q band at lower energy. Relative to the unsubstituted monomer, the Q and Soret bands of Ni(OEP-C_4SiMe_3) are shifted to lower energy and also broadened. In the dimer, the Soret band shows a further red shift and is also much broader, showing several distinct components. The intensity of the Q band is also enhanced in the dimer. The observed spectra of all three species are dominated by intense $\pi \rightarrow \pi^*$ transitions, and so emphasis throughout is placed on the ligand-based π levels. The simple model porphyrin Ni(P) has two closely spaced π levels in the occupied manifold and a vacant doubly degenerate π^* orbital. The butadiyne substituent selectively stabilizes one component of this degenerate unoccupied π^* orbital, and also destabilizes one of the occupied π orbitals. The net result is a reduction of the HOMO−LUMO gap in Ni(P-C_4H), consistent with the observed red shift of both Q and Soret bands. In the dimer Ni(P)(μ-C_4)Ni(P), symmetric and antisymmetric pairs of orbitals with significant amplitude on the bridging C_4 fragment are split by some 4000 cm^{-1} when the porphyrin rings are coplanar. These splittings vanish if the porphyrin rings are rotated into a staggered conformation, which lies approximately 15 kcal mol^{-1} higher than the coplanar ground state, indicating the presence of a considerable barrier to free rotation about the butadiyne axis. Both the broadening and red-shift of the Soret band in the dimer can be rationalized on the basis of the calculated one-electron transition energies, which in turn are determined by porphyrin−porphyrin coupling mediated by the butadiyne bridge.

Introduction

The porphyrins and their derivatives represent an important and diverse class of chromophores in biological systems,[1] most notably in light-harvesting pigments such as the chlorophylls, where the extended π system of the macrocycle provides a manifold of intense ligand $\pi \rightarrow \pi^*$ transitions in the visible region. In monomeric porphyrins, the resultant absorption envelope is typically relatively narrow, whereas efficient trapping of solar energy requires intense absorption over the whole visible region of the spectrum. In biological systems, the necessary broad-band absorption is achieved by grouping two or more chromophores together in close proximity,[2] resulting in a significant broadening of the visible absorption envelope. This strategy, in conjunction with the presence of several distinct pigments absorbing at different wavelengths, provides a highly successful mechanism for the gathering of sunlight.[3]

The synthesis of artificial chromophores containing more than one porphyrin center clearly has potential applications to biomimetic photosynthetic processes and is also relevant to more diverse fields such as liquid crystals,[4] nonlinear optics,[5] and molecular electronics.[6] Crossley and co-workers and other groups have developed a number of systems linked by fused aromatic rings,[7,8] where the enforced coplanarity of the rings ensures optimal overlap of porphyrin π systems. An alternative strategy for achieving significant inter-porphyrin coupling involves the use of unsaturated spacer groups such as phenyl,[9]

† Department of Chemistry, Faculties, The Australian National University.
‡ Queensland University of Technology.
§ University of Queensland.
|| Research School of Chemistry, The Australian National University.
⊗ Abstract published in *Advance ACS Abstracts,* November 15, 1996.

(1) (a) Dolphin, D., Ed. *The Porphyrins*, Academic Press: New York, 1978, and references therein. (b) Wasielewski, M. R. *Chem. Rev.* **1992**, *92*, 435−461.
(2) (a) Deisenhofer, J.; Epp, O.; Miki, K.; Huber, R.; Michel, H. *J. Mol. Biol.* **1984**, *180*, 385−398. (b) Deisenhofer, J.; Epp, O.; Miki, K.; Huber, R.; Michel, H. *Nature* **1985**, *318*, 618−624. (c) Allen, J. P.; Feher, G.; Yeates, T. O.; Komiya, H.; Rees, D. C. *Proc. Natl. Acad. Sci. U.S.A.* **1986**, *84*, 6162−6166.
(3) Voet, D.; Voet, J. G. *Biochemistry*; Wiley: New York, 1990.
(4) Gregg, B. A.; Fox, M. A.; Bard, A. J. *J. Am. Chem. Soc.* **1989**, *111*, 3024−3029.
(5) (a) Nalwa, H. S. *Adv. Mater.* **1993**, 341−358. (b) Anderson, H. L.; Sanders, J. K. M. *Angew. Chem., Int. Ed. Engl.* **1990**, *29*, 1400−1403.
(6) (a) McGhee, E. M.; Godfrey, M. R.; Hoffman, B. M.; Ibers, J. A. *Inorg. Chem.* **1991**, *30*, 803−808. (b) Lü, T. X.; Reimers, J. R.; Crossley, M. J.; Hush, N. S. *J. Phys. Chem.* **1994**, 98, 11878−11884.
(7) (a) Crossley, M. J.; Burn, P. L. *J. Chem. Soc., Chem. Commun.* **1991**, 1569−1571. (b) Crossley, M. J.; Burn, P. L. *J. Chem. Soc., Chem. Commun.* **1987**, 39−41.
(8) Kobayashi, N.; Numoa, M.; Kondo, R.; Nakajima, S.; Osa, T. *Inorg. Chem.* **1991**, *30*, 2241−2244.
(9) (a) Osuka, A.; Nakajima, S.; Nagata, T.; Maruyama, K.; Toriumi, K. *Angew. Chem., Int. Ed. Engl.* **1991**, *30*, 582−584. (b) Nagata, T.; Osuka, A.; Maruyama, K. *J. Am. Chem. Soc.* **1990**, *112*, 3054−3059. (c) Tabushi, I.; Sasaki, T. *Tetrahedron Lett.* **1982**, 1913−1916. (d) Sessler, J. L.; Johnson, M. R.; Creager, S. E.; Fettinger, J. C.; Ibers, J. A. *J. Am. Chem. Soc.* **1990**, *112*, 9310−9329. (e) Sessler, J. L.; Hugdall, J.; Johnson, M. R. *J. Org. Chem.* **1986**, *51*, 2838−2840. (f) Sessler, J. L.; Johnson, M. R.; Lin, T.-Y.; Creager, S. E. *J. Am. Chem. Soc.* **1988**, *110*, 3659−3661.

S0020-1669(96)01016-6 CCC: $12.00

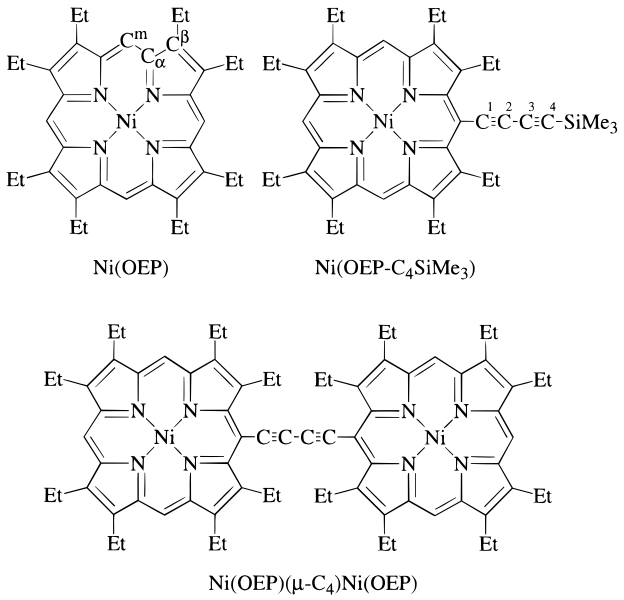

Figure 1. Molecular structures of Ni(OEP), Ni(OEP-C_4SiMe_3), and Ni(OEP)(μ-C_4)Ni(OEP).

biphenyl,[10] naphthyl,[11] and anthracenyl.[12] The dinickel(II) complex of *meso*,*meso*′-bis(octaethylporphyrinyl)butadiyne, [Ni(OEP)(μ-C_4)Ni(OEP)] (Figure 1), was first reported in 1978,[13] and since then we have described improvements to its synthesis.[14] In addition, the voltammetry and *in situ* spectroelectrochemistry of a series of four-coordinate homo- and heterobimetallic derivatives of this ligand have been reported.[15] Anderson and co-workers,[16] Therien and co-workers,[17] and Gosper and Ali[18] have prepared a variety of ethyne- and butadiyne-bridged systems, including a soluble decamer,[16] while we have developed routes to dimers in which the conjugated alkyne bridge is extended by the incorporation of other unsaturated moieties.[19] We have also recently reported the crystal structure of the Ni(OEP) dimer linked by 2,5-diethynylthiophene.[20] The spectra of all the *meso*-linked ethyne- and butadiyne-bridged species are characterized by a broad and intense absorption envelope in the visible region and hence fulfil the basic criteria for efficient light harvesting.

Several attempts have been made to rationalize the observed splitting of the Soret band, most notably the exciton coupling model developed by Kasha.[21] Within the limits of this model, the calculated Soret band splitting is independent of the nature of the bridging group. The substantial underestimation of the band splittings in butadiyne-bridged systems by the exciton coupling model suggests that covalent interactions mediated by the bridge may be crucial to the observed spectroscopic properties.[22] An alternative explanation of the Soret band fine structure was recently provided by Therien and co-workers,[17a] who speculated that vibronic modulation of the electronic levels, as a result of coupling to alkyne stretching modes, may be responsible for the observed splittings. Given these apparent contradictions, we have undertaken a theoretical study of a series of porphyrin species using approximate density functional theory (DFT)[23] with the aim of exploring the extent of electronic coupling between porphyrin rings in dimeric systems such as Ni(OEP)(μ-C_4)Ni(OEP). The computational efficiency of DFT relative to traditional *ab initio* techniques, which have previously been extensively used to study metalloporphyrin systems,[24] makes it an ideal tool for dealing with large systems, and several studies of metalloporphyrins and related species have emerged in the last few years.[25,26]

The observed spectroscopic properties of porphyrin systems are significantly influenced by configuration interaction (CI) between two closely spaced excited states,[27] a feature which is beyond the scope of current DFT methods.[28] However, for the dimeric species of interest here, a full CI treatment using conventional *ab initio* techniques is intractable due to the large size of the systems. In this contribution, we will therefore focus on the ground-state electronic structure of the porphyrins and use calculated one-electron transition energies only as a guide to the likely trends in spectroscopic properties. We consider three systems, Ni(OEP), the butadiyne-substituted species Ni(OEP-C_4SiMe_3), and dimeric Ni(OEP)(μ-C_4)Ni(OEP) (Figure 1). These three molecules represent a logical increase in complexity from the simple monomeric porphyrin Ni(OEP) through to the dimeric species. The butadiyne-substituted system represents an intermediate situation, where the influence of a bridging C_4 spacer can be assessed in isolation. Through a comparison of the ground state electronic structure of all three systems, we aim to delineate the effects of the spacer group from those of the second porphyrin ring and hence determine which features of the observed optical spectrum of Ni(OEP)-

(10) (a) Heiler, D.; McLendon, G.; Rogalskyj, P. *J. Am. Chem. Soc*. **1987**, *109*, 604−606. (b) Helms, A.; Heiler, D.; McLendon, G. *J. Am. Chem. Soc*. **1991**,*113*, 4325−4327.
(11) Osuka, A.; Maruyama, K. *J. Am. Chem. Soc*. **1988**, *110*, 4454−4456.
(12) Chang, C. K.; Abdalmuhdi, I. *J. Org. Chem*. **1983**, *48*, 5388−5390.
(13) Arnold, D. P.; Johnson, A. W.; Mahendran, M. *J. Chem. Soc., Perkin Trans 1* **1978**, 366−370.
(14) Arnold, D. P.; Nitschink, L. J. *Tetrahedron* **1992**, *48*, 8781−8792.
(15) Arnold, D. P.; Heath, G. A. *J. Am. Chem. Soc*. **1993**, *115*, 12197−12198.
(16) (a) Anderson, H. L. *Inorg. Chem*. **1994**, *33*, 972−981. (b) Anderson, H. L.; Martin, S. J.; Bradley, D. D. C. *Angew. Chem., Int. Ed. Engl*. **1994**, *33*, 655−658. (c) Anderson, H. L.; Sanders, J. K. M. *J. Chem. Soc., Chem. Commun*. **1989**, 1714−1715.
(17) (a) Lin, V. S.-Y.; DiMagno, S. G.; Therien, M. J. *Science* **1994**, *264*, 1105−1111. (b) Angiolillo, P. J.; Lin, V. S.-Y.; Vanderkooi, J. M.; Therien, M. J. *J. Am. Chem. Soc*. **1995**, *117*, 12514−12527.
(18) Gosper, J. J.; Ali, M. *J. Chem. Soc., Chem. Commun*. **1994**, 1707−1708.
(19) Arnold, D. P.; Nitschinsk, L. J. *Tetrahedron Lett*. **1993**, *34*, 693−696.
(20) Arnold, D. P.; James, D. A.; Kennard, C. H. L.; Smith, G. *J. Chem. Soc., Chem. Commun*. **1994**, 2131−2132.
(21) Kasha, M.; Rawls, H. R.; El-Bayoumi, M. A. *Pure Appl. Chem*. **1965**, *11*, 371−392.
(22) (a) Hunter, C. A.; Sanders, J. K. M.; Stone, A. J. *Chem. Phys*. **1989**, *133*, 395−404. (b) Eriksson, S.; Källebring, B.; Larsson, S.; Märtensson, J.; Wennerström, O. *Chem. Phys*. **1990**, *146*, 165−177. (c) Gouterman, M.; Holten, D.; Lieberman, E. *Chem. Phys*. **1977**, *25*, 139−153. (d) Koester, V. J.; Fong, F. K. *J. Phys. Chem*. **1976**, *80*, 2310−2312. (e) Tabushi, I.; Kugimiya, S.; Kinnaird, M. G.; Sasaki, T. *J. Am. Chem. Soc*. **1985**, *107*, 4192−4199.
(23) Ziegler, T. *Chem. Rev*. **1991**, *91*, 651−667.
(24) (a) Zwaans, R.; van Lenthe, J. H.; den Boer, D. H. W. *J. Mol. Struct*. **1995**, *339*, 153−160. (b) Rawlings, D. C.; Gouterman, M.; Davidson, E. R.; Feller, D. *Int. J. Quantum Chem*. **1985**, *28*, 773−842. (c) Merchan, M.; Orti, E.; Roos, B. O. *Chem. Phys. Lett*. **1994**, *221*, 136−144.
(25) (a) Case, D. A.; Karplus, M. *J. Am. Chem. Soc.* **1977**, *99*, 6182−6193. (b) Delley, B. *Physica B* **1991**, *172*, 185−193. (c) Jones, D. H.; Hinman, A. S.; Ziegler, T. *Inorg. Chem*. **1993**, *32*, 2092−2095. (d) Ghosh, A.; Almlöf, J. *Chem. Phys. Lett*. **1993**, *213*, 519−521. (e) Almlöf, J.; Fischer, T. H.; Gassman, P. G.; Ghosh, A.; Häser, M. *J. Phys. Chem*. **1993**, *97*, 10964−10970. (f) Ghosh, A.; Almlöf, J. *J. Am. Chem. Soc*. **1994**, *116*, 1932−1940. (g) Rosa, A.; Baerends, E. J. *Inorg. Chem*. **1994**, *33*, 584- 595.
(26) (a) Case, D. A. *Annu. Rev. Phys. Chem*. **1982**, 33, 151−171. (b) Daul, C.; Baerends, E. J.; Vernooijs, P. *Inorg. Chem*. **1994**, *33*, 3538−3543. (c) Stor, G. J.; Stufkens, D. J.; Vernooijs, P.; Baerends, E. J.; Fraanje, J.; Goubitz, K. *Inorg. Chem*. **1995**, *34*, 1588- 1594. (d) Rosa, A; Ricciardi, G.; Baerends, E. J.; Stufkens, D. J. *Inorg. Chem*. **1995**, *34*, 3425−3432.
(27) (a) Gouterman, M. *J. Chem. Phys*. **1959**, *30*, 1139−1161. (b) Gouterman, M. *J. Mol. Spectrosc*. **1961**, *6*, 138−163. (c) Weiss, C.; Kobayashi, H.; Gouterman, M. *J. Mol. Spectrosc*. **1965**, *16*, 415−450. (d) Gouterman, M. In ref 1, pp 1−166.
(28) Cook, M.; Karplus, M. *J. Phys. Chem*. **1987**, *91*, 31−37.

Table 1. Average Bond Lengths (Å) for Ni(P), Ni(P-C_4H), and Ni(P)(μ-C_4)Ni(P)[a]

bond	Ni(P)	Ni(P-C_4H)	Ni(P)(μ-C_4)Ni(P)	Ni(OEP)[35]
N−N	1.937	1.938	1.940	1.958
N−C^{α}	1.387	1.386	1.388	1.376
C^{α}−C^{β}	1.435	1.436	1.432	1.443
C^{β}−C^{m}	1.366	1.382	1.376	1.371
C^{m}−C^{1}		1.401	1.394	
C^{1}−C^{2}		1.220	1.222	
C^{2}−C^{3}		1.346	1.336	
C^{3}−C^{4}		1.216	1.222	

[a] Crystallographically determined values for Ni(OEP) are shown for comparison.

(μ-C_4)Ni(OEP) are truly a consequence of the dimeric nature of the complex.

Details of Experiments and Calculations

The Ni(OEP), Ni(OEP-C_4SiMe_3) and [Ni(OEP)(μ-C_4)Ni(OEP)] complexes were prepared by literature methods.[13,14] Electronic spectra were recorded in $CHCl_3$ on a Cary 3 spectrophotometer. The approximate density functional calculations reported in this work were performed using the Amsterdam Density Functional (ADF) package, Version 2.0.1, developed by Baerends and co-workers.[29] To simplify computations, the ethyl groups of the (OEP) unit were replaced by hydrogen atoms, as was the $SiMe_3$ group of Ni(OEP-C_4SiMe_3). An uncontracted double-ζ basis set, augmented with a single polarization function (p for H, d for C, N) was used for all main group atoms, while a triple-ζ basis set was used for Ni. Core levels up to 3p for Ni and 1s for both C and N were kept frozen during the calculations. Geometries of the model complexes Ni(P), Ni(P-C_4H), and Ni(P)(μ-C_4)Ni(P) were optimized using the gradient algorithms of Versluis and Ziegler[30] within D_{4h}, C_{2v}, and D_{2h} symmetry, respectively. For the optimization procedures, the LSD exchange-correlation potential was employed,[31] together with the Vosko-Wilk-Nusair parameterization of electron gas correlation.[32] Gradient corrections to the exchange (Becke)[33] and correlation (Perdew)[34] potentials were included in the calculation of ground and excited state energies. Reported excitation energies correspond to the difference in self-consistent total energies of the ground and excited states (ΔSCF method) and therefore incorporate the effects of electronic relaxation in the excited state.

Results and Discussion

Molecular and Electronic Structure of Ni(P), Ni(P-C_4H) and Ni(P)(μ-C_4)Ni(P). Optimized geometric parameters for Ni(P), Ni(P-C_4H) and Ni(P)(μ-C_4)Ni(P) are summarized in Table 1. Averaged crystallographic data from the triclinic structure of Ni(OEP) are also shown for comparison.[35] In the unsubstituted porphyrin, the calculated structural parameters are in excellent agreement with the experimentally determined ones, bond lengths lying within 0.02 Å in all cases. In Ni(P-C_4H), the butadiyne substituent produces only very minor distortions in the calculated porphyrin molecular architecture, the only significant change being a slight lengthening of the C_{α}−C_m bonds adjacent to the C_4H. The addition of a second porphyrin ring, giving Ni(P)(μ-C_4)Ni(P), results in only minor additional structural changes to both porphyrin and butadiyne fragments.

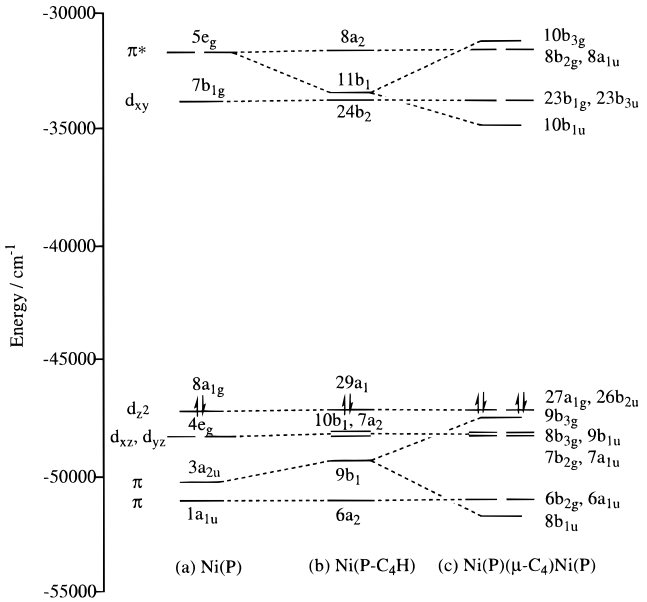

Figure 2. Comparative molecular orbital diagrams for Ni(P), Ni(P-C_4H), and Ni(P)(μ-C_4)Ni(P).

The energies of the valence orbitals of Ni(P), Ni(P-C_4H) and Ni(P)(μ-C_4)Ni(P) are summarized in Figure 2. The two highest occupied levels ($8a_{1g}$, $4e_g$) in Ni(P) are found to be Ni 3d-based orbitals, while the LUMO ($7b_{1g}$) is Ni-N σ antibonding. The highest lying ligand-based orbitals, $3a_{2u}$ and $1a_{1u}$, lie some 2000 cm^{-1} lower in energy than their metal-based counterparts. The relative ordering of metal- and ligand-based orbitals in metalloporphyrins has been the subject of some debate, extended Hückel calculations placing the metal-based levels above the ligand orbitals in Ni(P),[36] whereas the SCF−Xα−SW method results in the opposite ordering for Cu(P).[25a] More recently, approximate density functional calculations by Baerends and co-workers reported a very similar ordering of levels for Ni(P) to that given in Figure 2.[25g] The relative ordering of the orbitals in the ground state does not, of course, necessarily determine the nature of the ground state of the corresponding cation, due to the electronic and geometric relaxation which can occur upon ionization. Accordingly, we have optimized geometries of four possible cationic states, corresponding to removal of an electron from $8a_{1g}$, $4e_g$, $3a_{2u}$, and $1a_{1u}$ molecular orbitals. The ground state of $Ni(P)^+$ was found to arise from removal of an electron from the $3a_{2u}$ molecular orbital, indicating that $Ni(P)^+$ is best formulated as a ligand radical (Ni^{2+})($P^{\cdot+}$) rather than a Ni^{III} species (Ni^{3+})(P).

While the relative ordering of metal and ligand-based orbitals is clearly relevant to the electrochemical properties of the porphyrins, it is less crucial to the discussion of the electronic spectra of porphyrins. Electronic transitions involving metal-based orbitals do not contribute significantly to the optical spectrum, as evidenced by the remarkable similarity of the spectra of metalloporphyrins with widely varying central metal ions,[27] and the intense transitions are principally ligand $\pi \rightarrow \pi^*$ in nature. Therefore, the relative energies and orientations of the ligand-based π and π^* orbitals are of more direct significance to the spectroscopic properties of the neutral porphyrins. Contour plots of the highest occupied ($3a_{2u}$, $1a_{1u}$) and the lowest unoccupied ($5e_g$) ligand orbitals are shown in Figure 3. The most significant point to arise from Figure 3 is that while $3a_{2u}$ has a large contribution from pπ orbitals on the

(29) (a) Baerends, E. J.; Ellis, D. E.; Ros, P. *Chem. Phys.* **1973**, *2*, 42−51. (b) Baerends, E. J.; Ros, P. *Chem. Phys.* **1973**, *2*, 52−59. (c) Baerends, E. J.; Ros, P. *Int. J. Quantum. Chem.* **1978**, *S12*, 169−190.
(30) Versluis, L.; Ziegler, T. *J. Chem. Phys.* **1988**, *88*, 322−328.
(31) Parr, R. G.; Yang, W. *Density Functional Theory of Atoms and Molecules*; Oxford University Press: New York, 1989.
(32) Vosko, S. H.; Wilk, L.; Nusair, M. *Can. J. Phys.* **1980**, *58*, 1200−1211.
(33) Becke, A. D. *Phys. Rev. A* **1988**, *38*, 3098−3100.
(34) Perdew, J. P. *Phys. Rev. B* **1986**, *33*, 8822−8824.
(35) Cullen, D. L.; Meyer, E. F. Jr. *J. Am. Chem. Soc.* **1974**, *96*, 2095−2102.
(36) Antipas, A.; Gouterman, M. *J. Am. Chem. Soc.* **1983**, *105*, 4896−4901.

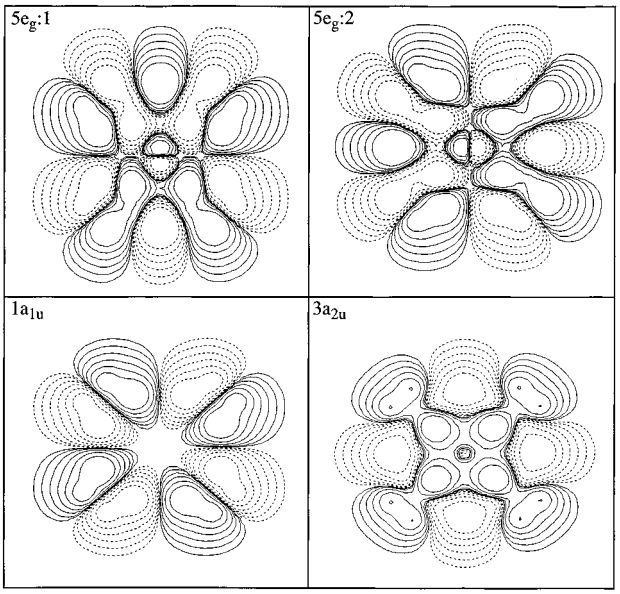

Figure 3. Contour plots of the $1a_{1u}$, $3a_{2u}$ (π), and $5e_g$ (π^*) orbitals of Ni(P). Plots are shown in a plane 1 Å above the atomic nuclei. Successive contours correspond to ±0.001, ±0.002, ±0.004, ±0.008, ±0.016, and ±0.032 (electrons/au^3)$^{1/2}$.

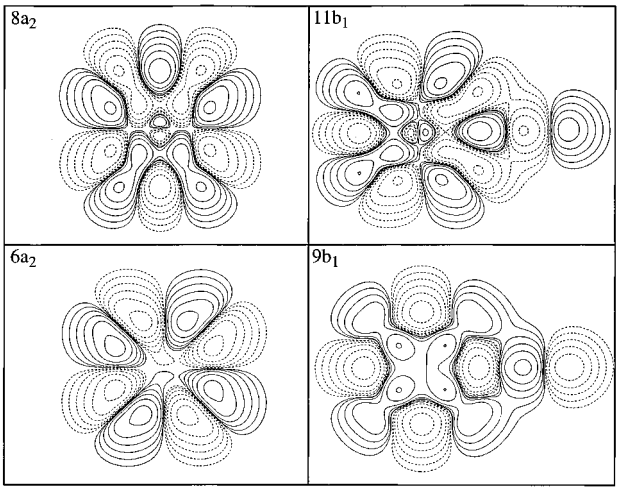

Figure 4. Contour plots of the $6a_2$, $8a_2$, $9b_1$, and $11b_1$ orbitals of Ni(P-C_4H). Successive contours are as in Figure 4.

meso carbons (C_m), $1a_{1u}$ has nodes at all four *meso* sites. Likewise, one component of the $5e_g$ orbital ($5e_g$:1) has significant amplitude on one pair of *trans*-oriented meso sites, while $5e_g$:2 is localized on the other pair. We can therefore anticipate that the two occupied orbitals and the also the two components of $5e_g$ will respond rather differently to the addition of a C_4H substituent at one *meso* site.

The descent in symmetry from D_{4h} [Ni(P)] to C_{2v} [Ni(P-C_4H)] results in a splitting of each doubly degenerate e_g level into orbitals of b_1 and a_2 symmetry, while the nondegenerate a_{2u} and a_{1u} orbitals correlate with b_1 and a_2, respectively. The pπ orbitals at the substituted *meso* site of the porphyrin transform as b_1, and consequently, only the b_1 porphyrin levels will be significantly influenced by the substituent. Accordingly, the $6a_2$ and $8a_2$ orbitals (derived from $1a_{1u}$ and $5e_g$:1 respectively) are essentially unaffected by the butadiyne fragment, while in contrast both $9b_1$ (derived from $3a_{2u}$) and $11b_1$ (derived from $5e_g$:2) orbitals have a significant contribution from the C_4 π system, and are shifted in energy relative to the corresponding orbitals in Ni(P). The important interactions between the porphyrin ring π system and that of the C_4 fragment are shown schematically in Figure 5. The $9b_1$ orbital is destabilized by

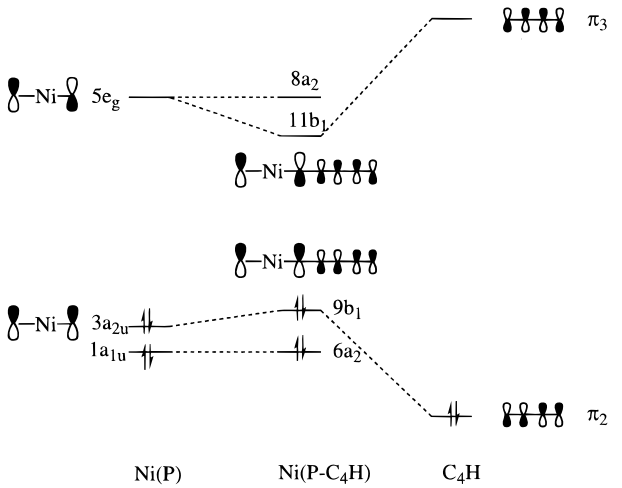

Figure 5. Interaction between the π systems of Ni(P) and butadiyne (C_4).

an antibonding interaction with the occupied π_2 orbital of butadiyne, while the higher-lying $11b_1$ is stabilized by a bonding interaction with a vacant π_3 orbital. The presence of a butadiyne substituent therefore reduces the gap between the highest occupied and lowest unoccupied ligand-based orbitals.

In comparing Ni(P-C_4H) with the dimeric species Ni(P)(μ-C_4)Ni(P), we note that each porphyrin-based orbital of the monomer will correlate with a pair of orbitals in the dimer, the splitting between the two members of the pair being indicative of the extent of communication between the porphyrin rings. It is clear from Figure 2c that only the b_1 orbitals of Ni(P-C_4H) are significantly split in the dimer, resulting in a considerable broadening within the manifolds of both occupied and unoccupied ligand-based orbitals and hence a further reduction in the ligand-based HOMO−LUMO gap. The $10b_{3g}$ and $10b_{1u}$ orbitals may be regarded as symmetric and antisymmetric combinations of $11b_1$ respectively, while $9b_{3g}$ and $8b_{1u}$ are the corresponding combinations of $9b_1$. The contour plots in Figure 6 show that the b_{1u} orbitals are bonding with respect to the central C−C bond, and are consequently lower in energy than their antibonding b_{3g} counterparts. The relationship of the ($10b_{3g}$, $10b_{1u}$) and ($9b_{3g}$, $8b_{1u}$) pairs to the $11b_1$ and $9b_1$ orbitals of Ni(P-C_4H), and hence to the $5e_g$:2 and $3a_{2u}$ orbitals of the parent monomer, can be clearly traced through Figures 3, 4, and 6. The orbitals derived from the a_2 orbitals of Ni(P-C_4H) remain unperturbed in the dimer, forming degenerate (b_{2g}, a_{1u}) pairs with no amplitude on the bridging butadiyne fragment.

In discussing the electronic structure of the dimeric species Ni(P)(μ-C_4)Ni(P), we have assumed throughout that the system adopts the coplanar conformation shown in Figure 1, as is the case in the 2,5-diethynylthiophene-bridged species.[20] There is of course no barrier to rotation about an isolated triple bond, an observation which has led Anderson to suggest that rotation of the two porphyrin rings about a butadiyne bridge should be equally facile.[16a] In contrast, Therien and co-workers have proposed that coplanarity of the porphyrin rings is necessary to explain the spectroscopic properties of mono/alkyne-bridged species.[17a] In phenyl and biphenyl bridged systems, free rotation about the C−C single bonds is prevented by steric interactions between the groups in the *ortho* positions. Accordingly, the porphyrin rings are coplanar in the phenyl-bridged system, and the Soret band is strongly split,[9b] while in the biphenyl systems, they lie perpendicular and the Soret band is narrow.[10b] The position of the conformational equilibrium is therefore a matter of considerable relevance to the forthcoming discussion of the spectroscopic properties of the dimer. Accordingly, the structure

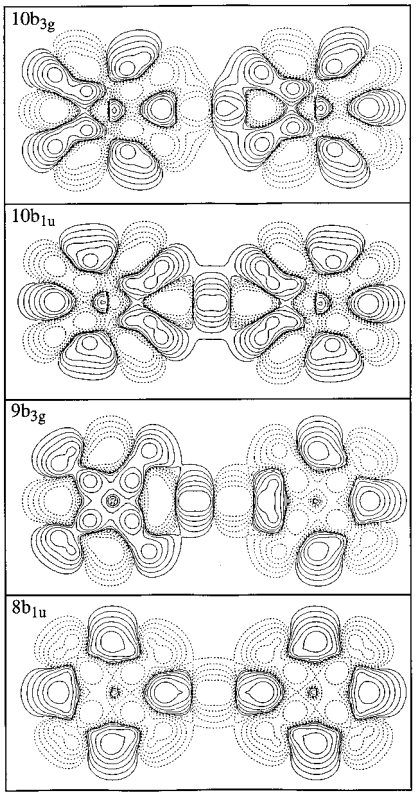

Figure 6. Contour plots of the $8b_{1u}$, $9b_{3g}$, $10b_{1u}$, and $10b_{3g}$ orbitals of Ni(P)(μ-C_4)Ni(P). Successive contours are as in Figure 4.

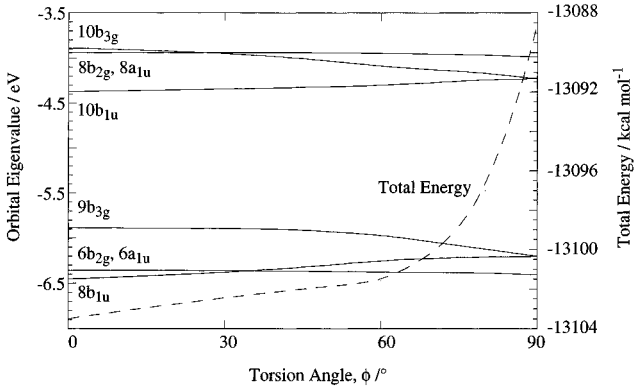

Figure 7. Walsh diagram showing the change in orbital and total energies as a function of torsion angle for Ni(P)(μ-C_4)Ni(P).

of the dimer was reoptimized with the porphyrin rings in a variety of conformations between the coplanar ($\phi = 0°$) and fully staggered ($\phi = 90°$) conformations. The variation in total energy as a function of torsion angle is illustrated in Figure 7, along with the eigenvalues of the ligand-based orbitals. The figure indicates that the total energy is relatively insensitive to rotations of $\pm 60°$ about the butadiyne axis, but rises rapidly near the staggered conformer, which lies approximately 15 kcal mol^{-1} higher in energy than the coplanar species. This estimate of the rotation barrier is an order of magnitude greater than the recently-reported value of Therien and co-workers using semiempirical methods.[37] In the experimental system, Ni(OEP)(μ-C_4)-Ni(OEP), steric repulsion between the ethyl groups will however destabilize the coplanar conformation to some extent, thereby reducing the rotation barrier. In view of the flatness of the calculated potential energy surface below $\phi = 60°$, it seems likely that these steric effects will cause significant librations about the central C−C bond, but not free rotation.

(37) Lin, V. S.-Y.; Therien M. J. *Chem. Eur. J.* **1995**, *1*, 645−651.

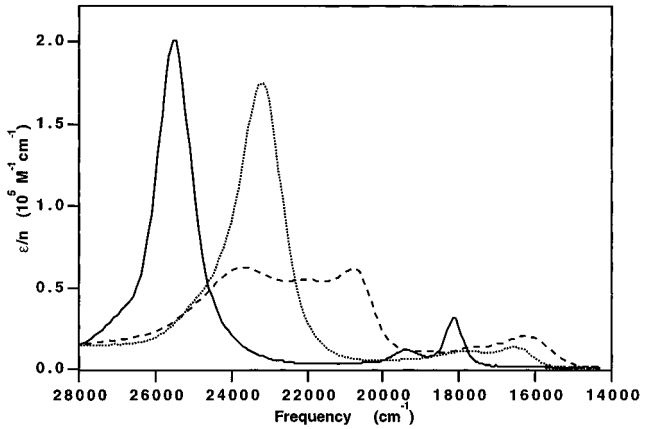

Figure 8. Visible absorption spectra ($CHCl_3$ solution) of Ni(OEP) (solid line), Ni(OEP-C_4SiMe_3) (dotted line), and Ni(OEP)(μ−C_4)Ni-(OEP) (dashed line) (plotted as extinction coefficient per porphyrin unit).

In terms of the analysis of the electronic spectrum, the most important aspect of this rotation is the effect it has on the splitting of the (b_{3g}, b_{1u}) pairs shown in Figure 2. Each pair correlates with a degenerate e level of the D_{2d} point group in the fully staggered limit, and consequently the one-electron splittings discussed above vanish where $\phi = 90°$. In the range where $\phi < 60°$, however, the separation of the b_{3g} and b_{1u} components is found to remain relatively constant, and the point at which the total energy begins to rise steeply corresponds to the point where the one-electron splittings collapse rapidly. Therefore the basic features of the molecular orbital diagram shown in Figure 2c will persist for relatively large ($-60° < \phi < 60°$) librations about the central C−C bond, but not for the fully staggered conformer.

Electronic Spectra of Ni(OEP), Ni(OEP-C_4SiMe_3), and Ni-(OEP)(μ-C_4)Ni(OEP). The electronic spectra of the three title compounds are shown in Figure 8. The spectrum of the monomer, Ni(OEP), is typical of that observed for metalloporphyrins,[1] with an intense Soret (B) band at 25 600 cm^{-1} and a weaker Q band at 18 200 cm^{-1}. The Q band typically consists of two distinct peaks, denoted $Q_{0,0}$ and $Q_{1,0}$, with the latter some 1000−1500 cm^{-1} to higher energy. The $Q_{1,0}$ absorption is normally assigned as a vibronic sideband off the Q band electronic origin $Q_{0,0}$.[22c,38] In Ni(OEP-C_4SiMe_3), both the Soret and Q bands are red-shifted relative to the unsubstituted species, appearing at approximately 23 000 and 16 500 cm^{-1}, respectively. Both Q and Soret bands are noticeably broader than those in Ni(OEP), although no distinct splittings can be identified. In the related *p*-nitrophenyl-substituted species Ni(OEP-C_4-$C_6H_4NO_2$), however, the Soret band is distinctly split, one component being highly solvent-dependent.[39] In the dimer, a further red shift of both Soret and Q bands is observed, along with a considerable increase in the intensity of the Q band relative to that of the Soret region. In addition, whereas only a single Soret band is observed in the spectra of both monomers, a broad multiplet structure is evident in the dimer.

Calculated one-electron transition energies for the electric dipole-allowed $\pi \rightarrow \pi^*$ transitions of Ni(P), Ni(P-C_4H) and Ni(P)(μ-C_4)Ni(P) are summarized in Table 2 and graphically shown in Figure 9. The transitions of the latter two are grouped in such a way as to emphasize their relationship to those of the

(38) (a) Eaton, W. A.; Hochstrasser, R. M. *J. Chem. Phys.* **1967**, *46*, 2533−2539. (b) Eaton, W. A.; Hochstrasser, R. M. *J. Chem. Phys.* **1968**, *49*, 985−995.

(39) Imahori, H.; Higuchi, H.; Matsuda, Y.; Itagaki, A.; Sakai, Y.; Ojima, J.; Sakata, Y. *Bull. Chem. Soc. Jpn.* **1994**, *67*, 2500−2506.

Table 2. Calculated One-Electron Transition Energies (cm^{-1}) for Ni(P), Ni(P-C_4H), and Ni(P)(μ-C_4)Ni(P)

Ni(P)			Ni(P-C_4H)			Ni(P)(μ-C_4)Ni(P)		
transition	energy	state	transition	energy	state	transition	energyy	state
$3a_{2u} \rightarrow 5e_g$	18 900	E_u	$9b_1 \rightarrow 11b_1$	16 400	A_1	$9b_{3g} \rightarrow 10b_{1u}$	12 500	B_{2u}
						$8b_{1u} \rightarrow 10b_{3g}$	20 900	B_{2u}
			$9b_1 \rightarrow 8a_2$	18 800	B_2	$9b_{3g} \rightarrow 8a_u$	16 300	B_{3u}
						$8b_{1u} \rightarrow 8b_{2g}$	20 600	B_{3u}
$1a_{1u} \rightarrow 5e_g$	19 800	E_u	$6a_2 \rightarrow 11b_1$	18 300	B_2	$6b_{2g} \rightarrow 10b_{1u}$	16 300	B_{3u}
						$6a_u \rightarrow 10b_{3g}$	20 200	B_{3u}
			$6a_2 \rightarrow 8a_2$	20 000	A_1	$6b_{2g} \rightarrow 8a_u$	19 700	B_{2u}
						$6a_u \rightarrow 8b_{2g}$	19 700	B_{2u}

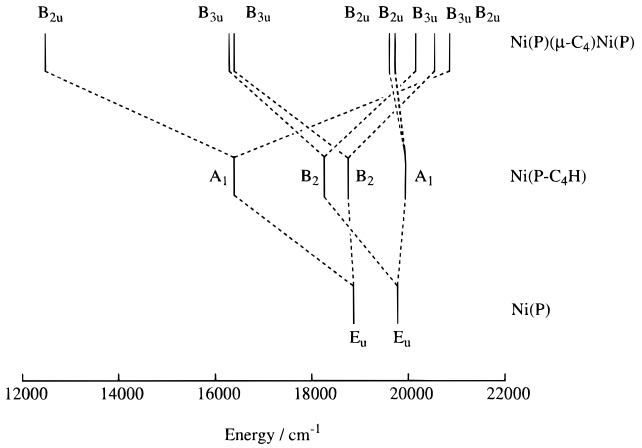

Figure 9. Calculated one-electron transition energies for Ni(P), Ni(P-C_4H), and Ni(P)(μ-C_4)Ni(P).

parent monomer, Ni(P). The reported values are taken from spin-restricted calculations and hence represent weighted averages of spin singlet and triplet excitations. Separate singlet and triplet transition energies were not calculated, as the singlet−triplet splittings in transitions between ligand-based orbitals have been shown to be relatively small in other porphyrin systems.[25a,g]

In the past, the Gouterman four-orbital model[27] has been extensively used to assign the Q and Soret band regions of the spectra of porphyrins. The basis of this model lies in the near degeneracy of the excited states of E_u symmetry arising from the $1a_{1u} \rightarrow 5e_g$ and $3a_{2u} \rightarrow 5e_g$ transitions. Configuration interaction mixes these two excited states, influencing the spectrum in two ways. First, the two transitions are split about their barycenter, resulting in Soret and Q bands at higher and lower energy respectively, and second, the intensity of the Soret band is strongly enhanced at the expense of the Q band. In marked contrast to the porphyrins, the spectra of the related phthalocyanines[40] have Q and Soret bands of comparable intensities. Approximate DFT calculations confirm that in these systems the occupied a_{1u} and a_{2u} ligand-based orbitals are much further apart than in the porphyrins,[25g] and as a result the influence of CI is much reduced.

Since CI effects cannot be accounted for in density functional calculations, the computed $3a_{2u} \rightarrow 5e_g$ and $1a_{1u} \rightarrow 5e_g$ transition energies can at best estimate the *barycenter* of the $\pi \rightarrow \pi^*$ transitions.[25a] The calculated one-electron energies of the $3a_{2u} \rightarrow 5e_g$ and $1a_{1u} \rightarrow 5e_g$ transitions for Ni(P) lie within 900 cm^{-1} of each other, with a barycenter at 19 350 cm^{-1}. The observed centroid of the Soret and $Q_{0,0}$ bands occurs at 21 900 cm^{-1}, indicating that the DFT results reproduce the experimental barycenter of the $\pi \rightarrow \pi^*$ manifold to within 2500 cm^{-1}. The observed splitting between Q and Soret bands is, however, 7400 cm^{-1} compared to the calculated one-electron separation of only 900 cm^{-1}. The CI between the two closely spaced states therefore contributes 6000−7000 cm^{-1} to the observed band splittings. Equipped with these general conclusions regarding the performance of the DFT method and the influence of CI, we are now in a position to draw some general conclusions regarding the appearance of the spectra of the more complex species.

The most notable feature of the spectrum of Ni(OEP-C_4-$SiMe_3$) is its striking similarity to Ni(OEP), indicating that CI retains a significant role in determining the band positions and intensities. The reduction from D_{4h} to C_{2v} symmetry splits the degeneracy of both E_u $\pi \rightarrow \pi^*$ transitions, resulting in two excited states of A_1 symmetry and two of B_2 symmetry (Figure 9). The $9b_1 \rightarrow 11b_1$ (A_1) transition is strongly red-shifted, $9b_1 \rightarrow 8a_2$ (B_2) and $6a_2 \rightarrow 11b_1$ (B_2) are also red-shifted but to a lesser extent, while $6a_2 \rightarrow 8a_2$ (A_1) is virtually unperturbed from its position in Ni(P). The barycenters of the A_1 and B_2 pairs lie within 300 cm^{-1} of each other at approximately 17 800 cm^{-1}, indicating that the net influence of the butadiyne substituent is to shift the $\pi \rightarrow \pi^*$ manifold approximately 1500 cm^{-1} to lower energy relative to Ni(P), consistent with the experimentally observed red-shift of both Q and Soret bands.

The CI between the two A_1 and two B_2 states will result in two distinct components in both Q and Soret bands, and so it is at first sight somewhat surprising that the reduction in symmetry from D_{4h} [Ni(OEP)] to C_{2v} [Ni(OEP-C_4SiMe_3)] symmetry results only in a broadening of the Q and Soret bands rather than a distinct splitting. However, we note that if the transitions are accompanied by negligible relaxation effects, the one-electron energies are given simply by the difference in ground-state orbital energies. In this case, the barycenters of the A_1 and B_2 pairs are necessarily coincident (see Figure 2). It is then necessary only to postulate that CI will be more significant between the closely spaced B_2 states than their counterparts of A_1 symmetry to conclude that the Q and Soret components of A_1 and B_2 symmetry will also be nearly degenerate. This accidental degeneracy clearly depends critically on the coincidence of the barycenters of the one-electron transition energies of each symmetry which arises only in the absence of electronic relaxation in the excited states. If the transition is accompanied by a significant redistribution of charge, the one-electron transition energies will no longer be given simply by the difference in ground-state orbital energies. Relaxation effects will be more significant in states of B_2 symmetry, where donor and acceptor orbitals are located in different areas of the molecule (Figure 4), and hence the barycenters of the A_1 and B_2 multiplets will diverge. This is consistent with the distinct splitting observed in the related *p*-nitrophenyl-substituted species Ni(OEP-C_4-$C_6H_4NO_2$),[39] where the electron-withdrawing nitro group will introduce significant charge-transfer character into the optical spectrum.

In the dimeric species, the two A_1 excited states of Ni(P-C_4H) split into four distinct B_{2u} states, while the monomer B_2 states give rise to four of B_{3u} symmetry. The separations between these states are determined by the splitting of the donor

(40) Edwards, L.; Gouterman, M. *J. Mol. Spectrosc.* **1970**, *33*, 292−310.

and acceptor orbitals shown in Figure 2. Accordingly, the two B_{2u} states arising from the lowest energy A_1 state of Ni(P-C_4H) are split by some 8400 cm^{-1}, while those arising from the higher energy A_1 state remain almost unperturbed in the dimer. The splitting of both monomer B_2 states is intermediate between these two extremes, the resultant B_{3u} components being separated by approximately 4000 cm^{-1}. The total manifold of one-electron $\pi \rightarrow \pi^*$ transitions spans 8400 cm^{-1} as opposed to 3600 and 900 cm^{-1} in Ni(P-C_4H) and Ni(P), respectively. Furthermore, five distinct excited states are clustered within a 1200 cm^{-1} window centered on 20300 cm^{-1}, and thus even without a consideration of the effects of CI, we can readily understand the multiplet structure of the Soret band. Unlike the comparison between Ni(P) and Ni(P-C_4H), there is no overall shift in the barycenter of the $\pi \rightarrow \pi^*$ manifold in going to the dimeric species. The distinct red-shift of the Soret band is therefore due to the splitting of the (b_{3g},b_{1u}) orbital pairs rather than a bulk shift in either the π or π^* manifolds.

Although the likely influence of CI is less easily predicted in the presence of eight distinct one-electron states, we can draw some general conclusions. First, the lowest energy excited state (B_{2u}) lies some 7000 cm^{-1} below the next state of the same symmetry, and will therefore be relatively unaffected by CI. Accordingly, the $9b_{3g} \rightarrow 10b_{1u}$ transition is a strong candidate for the leading band at 16 000 cm^{-1}. The reduced CI also leads directly to a prediction of increased Q-band intensity, consistent with the observed spectrum, although additional intensity in this region may also arise due to Q-band components arising from CI between the two B_{3u} states centered at 16 300 cm^{-1}. The Soret band region will feature components arising from CI between the five distinct transitions found above 19 700 cm^{-1}, as well as the Soret component of the B_{3u} states centered at 16 300 cm^{-1}. Although we cannot associate any specific Soret-band feature to a particular transition, the overall splitting of the band is clearly intimately linked to the one-electron splittings shown in Figure 9. It is noteworthy in this context that these one-electron splittings vanish in the staggered dimer, suggesting that in the absence of a significant barrier to rotation about the butadiyne axis, the Soret band would be considerably narrower than is observed.

Concluding Remarks

Throughout this work we have used approximate density functional theory to analyze the electronic structure and spectroscopic properties of a series of related nickel porphyrin species. The three complexes, Ni(OEP), Ni(OEP-C_4SiMe_3), and Ni(OEP)(μ-C_4)Ni(OEP), represent a logical structural progression from a simple monomeric metalloporphyrin to a bridged dimer system, where the lower prevailing symmetry and inter-porphyrin coupling complicate the analysis of the spectrum. The butadiyne-substituted monomer represents an intermediate situation where the effects of the bridging moiety can be analyzed in isolation.

The ligand-based molecular orbitals of the monomeric porphyrin, Ni(P) are typical of a metalloporphyrin. Two occupied porphyrin π orbitals lie within 1000 cm^{-1} of each other, and approximately 20 000 cm^{-1} below the doubly degenerate ligand π^* LUMO. In Ni(P-C_4H), the π orbitals of the butadiyne fragment interact with the porphyrin π system, destabilizing the ligand HOMO and stabilizing one component of the LUMO. The net result is a reduction in the ligand-based HOMO−LUMO gap, and therefore a distinct red-shift in the manifold of $\pi \rightarrow \pi^*$ transitions. Despite the reduction in symmetry, the Q and Soret bands are only broadened rather than showing distinct splittings. This somewhat surprising observation arises because, in the absence of significant charge-transfer character in the excited states, the barycenters of the A_1 and B_2 manifolds remain close together. Where the charge-transfer character is enhanced, for example by the presence of a *p*-nitrophenyl substituent on the butadiyne fragment, the $\pi \rightarrow \pi^*$ manifold is more strongly split, and the Soret band shows distinct multiplet character.

In the presence of a second porphyrin group, the A_1 and B_2 states of Ni(P-C_4H) correlate with states of B_{2u} and B_{3u} symmetry respectively. The lower energy A_1 state is split by 8400 cm^{-1} in the dimer and both B_1 states are split by 4000 cm^{-1}, while the higher energy A_1 state is virtually unperturbed. All these splittings collapse in the staggered conformer, which lies some 15 kcal mol^{-1} higher in energy. There are now eight electric dipole-allowed excited states to consider, spread over a range of 8400 cm^{-1} in the coplanar conformer. A particularly high density of states is found in the high energy (Soret band) region of the $\pi \rightarrow \pi^*$ manifold, with five distinct one-electron states occupying a 1200 cm^{-1} window. Thus both the multiplet structure of the Soret band and its distinct red shift can be qualitatively explained on the basis of splittings in the one-electron transition energies, which in turn are dictated by porphyrin−porphyrin coupling *via* the butadiyne bridge. This observation has important consequences for the design of light-harvesting chromophores, as it implies that increased coupling between the porphyrin centers may lead directly to a broader absorption window.

Acknowledgment. The financial support of the Australian Research Council to both R.S and D.P.A. is gratefully acknowledged.

IC961016M